13

Bearings Fault Detection Using Inference Tools

Miguel Delgado Prieto, Jordi Cusidó i Roura and
Jose Luis Romeral Martínez
MCIA Group, Technical University of Catalonia
Spain

1. Introduction

Electric motors are nowadays widely used in all kind of industrial applications due to their robustness and ease of control through inverters. Therefore, any effort, with the aim of improving condition monitoring techniques applied to them, will result in a reduction of overall production costs by means of productive lines stoppage reduction, and increment of the industrial efficiency. In this context, the most used electric machine in the industry is the Induction Motor (IM), due to its simplicity and reduced cost. The analysis of the origin of IMs failures exhibits that the bearings are the major source of fault (Singh et al., 2003), and even a common cause of degradation in other kinds of motors as Permanent Magnet Synchronous Machines. An IM failures percentage distribution, according to previous studies (O'Donell, 1986), is shown in figure 1, in order to highlight the bearings monitoring importance.

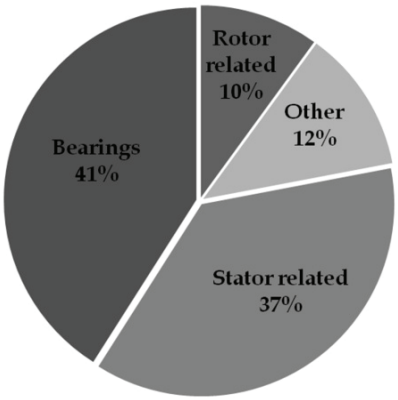

Fig. 1. IM failures percentage distribution.

Focusing in bearings defects, these have been typically categorized as distributed or local. Distributed defects include mainly surface roughness, waviness and misaligned races. Localized defects, however, include cracks, pits and spalls basically.
A great deal of studies concentrate their efforts in localized defects detection, because these defects are generally related with concrete fault indicators in the acquired signals, meanly

characteristics faults harmonics in machine vibrations. However, the issue related with the capability to detect both, localized and generalized bearings faults, is an important issue that should be attended (Cusido et al., 2009). Generalized degradation is difficult to detect because the lack of consistent characteristic fault harmonics in the spectral decomposition of any acquired signal. Therefore, it is difficult to inspect deeply motor bearings by analysing only some specific fault harmonics due to fault signal complexity (Obaid et al., 2003), and in the case of asynchronous motors the slip factor introduces additional difficulty. This fact makes necessary the diagnosis support of additional signal analysis (Frosini et al., 2008). The current trends in condition monitoring are related with the fusion of different features, which provide the possibility to merge fault indicators from different physical magnitudes (Cusido et al. 2010). This data fusion improves the diagnostic reliability, because fault indicators that are not descriptive enough themselves can contribute to detect faults in relation with others, especially if the features are extracted from different physical magnitudes, which enhance the monitoring capabilities. However, it is necessary to find the best and most useful fault indicators, and merge them by some kind of inference tool.
In this chapter, additional bearings fault features are introduced to be merged with traditional vibrations fault indicators. Hence, features from machine vibration, stator currents, stator common mode currents and acoustic emissions, are presented and related with bearing faults. With all these fault indicators diagnosis different systems based on multidimensional features fusion can be implemented. The bearing diagnosis capability and reliability are easily increased making possible the bearing fault detection even if the fault is localized or generalized. Regarding the inference tools for features fusion, it can be chosen a wide variety of methods such as statistical rules, expert systems or artificial intelligent techniques among others. In this chapter, two different inference tools are presented in order to generate two different diagnosis systems: Look-up tables, representing one of the easiest ways to merge information, and Fuzzy logic as a next step towards advanced diagnosis systems based on artificial intelligence.

2. Basic theory

A brief introduction of each proposed physical magnitude for bearings fault detection is presented next, with special attention to the specific bearings fault indicators.

2.1 Vibration analysis

Vibration analysis is one of the most extended condition monitoring techniques. Despite being a reliable, well studied robust technique, it requires that the motor under test has a vibration transducer installed. The measurements should be taken on the bearings, bearing support housing, or other structural parts that significantly respond to the dynamic forces and characterize the overall vibration of the machine. Therefore, the major disadvantage of vibration monitoring is that requires access to the machine, and specific accelerometers housing over the machine is sometimes required. For accurate measurements, sensors should be mounted tightly on the machine, and expertise is required in the mounting, condition that makes its online application expensive. Sometimes, other techniques without this kind of restriction are preferred or required.
The single-point bearing defects imply certain characteristic fault frequencies which will appear in the machine vibrations. The frequencies are predictable and depend on which surface of the bearings contains the fault. There is one characteristic fault frequency

associated with each of the four parts of the bearing. Vibration frequency components related to each of the four basic fault frequencies; (1) Fundamental train frequency, (2) Ball-spin frequency, (3) Ball pass outer race and (4) Ball pass inner race, can be calculated using the following expressions (Bellini et al., 2008):

$$FTF = \frac{1}{2} f_r \left(1 - \frac{P_d}{B_d}\right) \tag{1}$$

$$BSF = \frac{1}{2}\frac{P_d}{B_d} f_r \left[1 - \left(\frac{B_d}{P_d} cos\emptyset\right)^2\right] \tag{2}$$

$$BPFO = \frac{n}{2} f_r \left(1 - \frac{B_d}{P_d} cos\emptyset\right) \tag{3}$$

$$BPFI = \frac{n}{2} f_r \left(1 + \frac{B_d}{P_d} cos\emptyset\right) \tag{4}$$

with:

n: Number of bearing balls
fr: Rotor speed
Bd: Ball diameter
Pd: Bearing Pitch diameter
β: Contact angle of the ball on the race

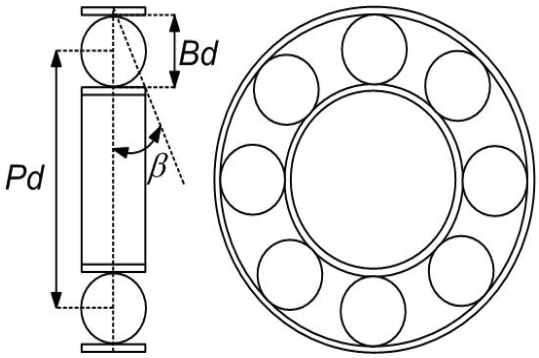

Fig. 2. Main bearing design parameters, B_d: ball diameter, P_d: pitch diameter, β: contact angle.

Regarding the roughness bearings defects, there is a wide variety of causes from contamination of the lubricant to the shaft currents or misalignment. The generalized roughness faults produce unpredictable broadband effects in the machines vibration spectrum, but it seems to be feasible the detection by means of the temporal vibration signal Root Mean Square (RMS) analysis. As some works and standards (Riley et al., 1999; Cabanas et al., 1996) set out, a RMS vibration value evaluation of the motor also provides a good indicator for motor health, allowing machine overall fault diagnosis.

2.2 Stator currents

A Motor Current Signature Analysis (MCSA) represents by the stator currents acquisition an interesting alternative method with its own particularities and benefits (Cusido et al., 2007a); the most interesting of them is to avoid accessing inside the motor making it easy to perform

its online fault analysis (Cusido et al. 2007b). It has been demonstrated (Schoen et al., 1995) that the characteristic bearing fault frequencies in vibration can be reflected on stator currents. As a result of motor airgap length variations due to bearings defect, flux density is influenced and then an additional magnetic flux appears. This magnetic flux, and its variations associated to rotor turning, creates additional components that can be found in the stator currents spectra (Cusido et al., 2005). Using this method it has been widely demonstrated in the literature (El Hachemi Benbouzid, 2000) that different faults like eccentricity, rotor asymmetry, stator winding failures, broken bars and bearings damage can be diagnosed. The relationship between the vibration frequencies and the current frequencies for bearing faults can be described by equation (5). Therefore, by means of (5), it is possible to analyze the specific fault harmonics in order to find abnormalities in their amplitude values.

$$f_{bg} = |f_e \pm m * f_v| \tag{5}$$

with:

f_{bg}: Electrical fault characteristic frequency
m: Integer
f_e: Electrical supply frequency
f_v: Vibration fault characteristic frequency {(1), (2), (3) or (4)}

It is well established that for bearing single-point defects, the characteristic stator current fault frequencies are good fault indicators. Even so, it was discovered in several studies, that for many in situ generated bearing faults, those characteristics fault frequencies are not observable and may not exist at all in stator current (Stack et al., 2004.). But it is demonstrated also that these same bearings faults have an effect over the motor eccentricity (Basak et al., 2006), and these characteristics stator current faults frequencies are easily detectable as sidebands over the fundamental motor current frequency. Therefore, the evaluation of the bearings characteristics stator current faults frequencies is useful for diagnosis proposes, because it can diagnose directly the bearing fault. But as a second diagnosis step, the analysis of stator current fundamental sidebands, in order to detect eccentricity, can be useful also for bearing diagnosis. However, it is necessary other fault indicators in order to classify correctly between eccentricity fault caused by bearing fault or eccentricity fault caused by other faults in the motor.

Regarding generalized bearing defects, previous works have shown the existing correlation between vibration and currents RMS values (Riley et al., 1999). Although it is a complex function that relates both magnitudes, this work tries to check the RMS currents reliability in order to perform the motor status diagnose.

2.3 High frequency common-mode pulses

One of the biggest culprits for bearings failure are common-mode circulating currents (CMC). The CMC are generated due to the inverter used to manage motors, because the inverter creates common mode voltage as figure 3 shows. Each high dv/dt over the inverter modulation implies a proportional current, which is propagated over the motor trough different paths to the ground in order to turn back to the inverter (Muetze and Binder, 2007a).

The CMC travels around the motor (and load if it is not electrically isolated), due to the capacitive effect that two conductive materials separated by means of some isolating material (dielectric) can create. For instance, the capacitive effect produced between the coil group and the chassis separated with air gaps in an induction motor.

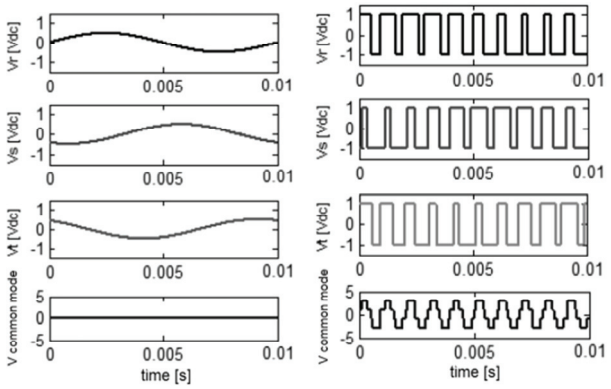

Fig. 3. Common mode voltage generated with PWM modulation.

The capacitances created inside the motor have a very low value, so the motor intrinsically gets filter the low frequency currents, but the high frequency currents see low impedance paths (Binder and Muetze, 2008.). Some current travel over the shaft, that in an electrical sense, find the bearing rail, lubricant and bearing ball capacitive coupling. The high frequency CMC pulses current that contain an important amplitude value, provoke a discharge over the capacitive coupling. This phenomenon is called EDM (Electric Discharge Machining) (Kar and Mohanty, 2008). The CMC influences on the bearings degradation due to the effect that every CMC discharge provoke over the lubricant that recover the bearing, because the continually application of these discharges implies lubricant degradation. This effect increases the contact between the bearings with the rail accelerating the final bearings degradation.

As it is shown in figure 4a, circulating currents could follow different paths to the ground through the stator windings or rotor. One important path of the circulating currents is through the bearings (Muetze and Binder, 2007b). The electrical scheme of parasitic capacitive couplings is shown also in figure 4b. This scheme represents the CMC path from inverter to bearings. As it has been explained previously, the inverter generates common mode voltage (V_{mc}) and at the same time, generates common mode current (I_{mc}) which is propagated trough the wire (L_C), motor (L_m) and through the coupling effect between the motor and chassis, and between the motor and rotor, this last ones cross finally the coupling effect between the shaft and the bearings.

A temporal CMC acquisition and a single common-mode discharge are shown in figure 5. These currents typically show a frequency range of mega-hertz with a period of micro-seconds between bursts. CMC discharges provoke bearings lubricant degradation. This effect provokes the contact between the bearings with the rail. Therefore, CMC discharges amplitude is directly depending of the parasitic capacitances which are depending of the lubricant state and the distance between bearings and rail mainly. Therefore, seems to be possible the bearings diagnosis by means of the number of CMC pulses that surpassed a prefixed amplitude threshold during a fixed time, in order to distinguish between fault and healthy bearings (Delgado et al., 2009). Analyzing the number of CMC pulses that surpassed a current amplitude threshold value, it is possible to see that a minor number of CMC pulses surpassing the threshold, is significant of a degradation state of the bearings, because the capacitive effect rail-lubricant-bearing needs a minor "*energy*" differential to allow an EDM.

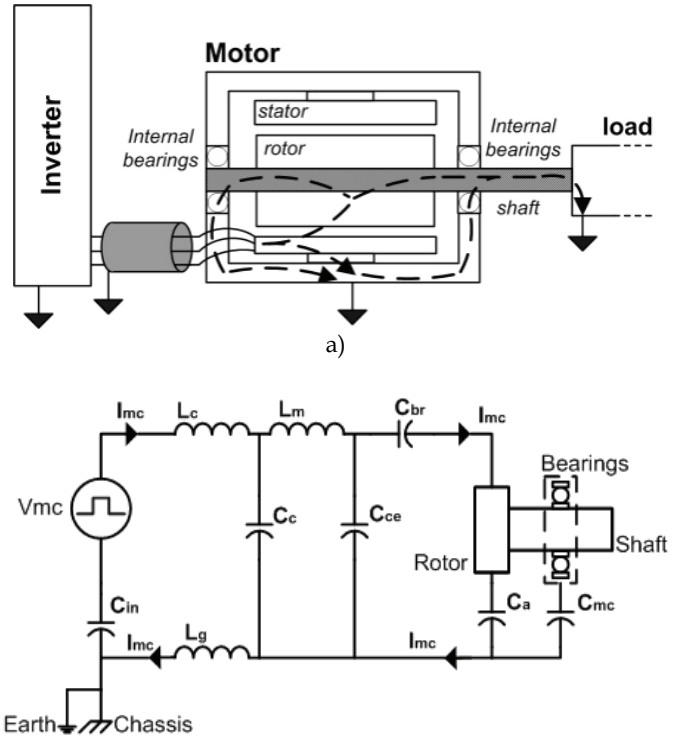

Fig. 4. a) Main CMC paths over inverter-motor-load system. b) Electrical Scheme for capacitive and parasitic couplings.

Therefore, the methodology consists in a first time acquisition over the stator CMC in a test bench with healthy bearings. The amplitude of the CMC pulses decrease at the same time that bearings degradation increase, so is necessary to specify a CMC pulses amplitude threshold and count the number of pulses that surpasses this threshold during a fixed time. Obviously, the time acquisition and the threshold value make depends the number of CMC pulses counted. An acquisition time of tens of milliseconds, and a threshold over the 75% of the maximum CMC pulses amplitude over healthy bearing, is enough to distinguish between healthy and degraded bearings.
In this work, to limit the CMC acquired signal to only pulses flowing through bearings (the responsible of balls degradation), a motor modification was introduced. All the ball bearing under test were isolated from the motor stator frame but in a point connected to ground through a cable where the pulses were measured. Bearings insulation was achieved by surrounding the piece with a polytetrafluoroethylene (PTFE) flat ring with a hole mechanized in it to let the cable pass through.

2.4 Acoustic Emissions

The Acoustic Emission Technique is a very promising tool that has practical application in several fields, and specifically, recent important relevance in condition monitoring of

machines. Acoustic Emission is defined as a radiation of mechanical elastic waves produced by the dynamic local rearrangement of the material internal structure. This phenomenon is associated with cracking, leaking and other physical processes and was described for the first time by Josef Kaiser in 1950. He described the fact that no relevant acoustic emission was detected until the pressure applied over the material under test surpassed the previously highest level applied.

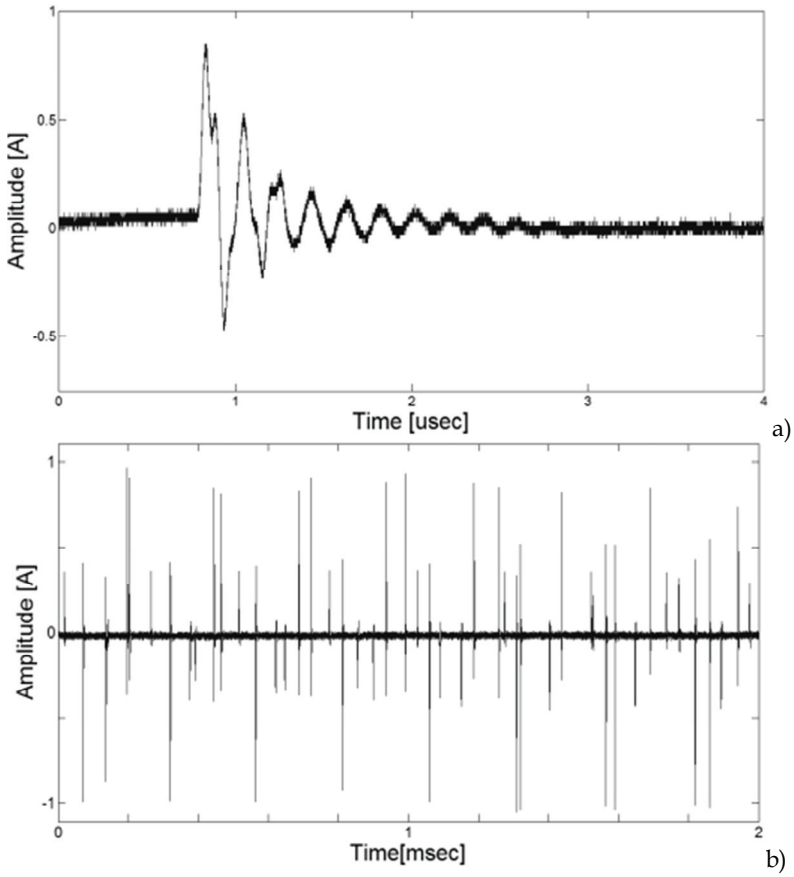

Fig. 5. Examples of common-mode current discharges, a) individual discharge, b) a set of discharges.

Acoustic Emissions Technique is classified as a passive technique because the object under test generates the sound and the Acoustic Emission sensor captures it. By contrast, Active methods rely on signal injection into the system and analysis of variations of the injected signal due to system interaction. Then an acoustic emission sensor captures the transient elastic waves produced by cracking or interaction between two surfaces in relative motion and converts their mechanical displacement into an electrical signal. This waves travel through the material in longitudinal, transverse (shear) or surface (Rayleigh) waves, but the majority of sensors are calibrated to receive longitudinal waves. Wherever the crack is

placed, the signal generated travels from the point of fracture to the surface of the material. The transmission pattern will be affected by the type of material crossed and then isotropic material will lead to spherical wave front types of propagation only affected by material surfaces or changes, where the Snell law rules their reflection and reflexion. On Figures 6 and 7 is shown the evolution of acoustic waves inside a Material. On figure 6 it is shown how reflections on waves due to the defect appear.

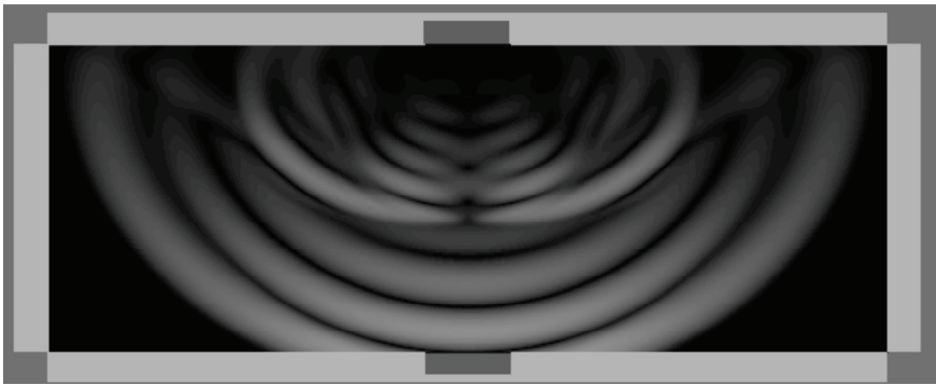

Fig. 6. Acoustic Emission Wave Propagation

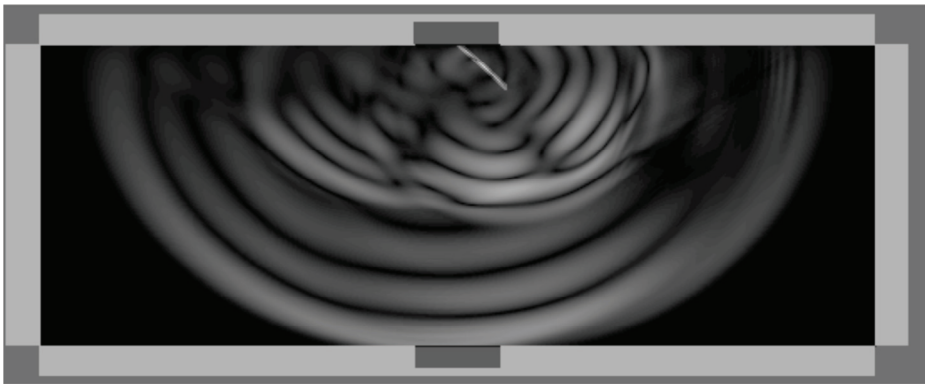

Fig. 7. Acoustic Emission Wave Propagation in fractured Material

The biggest advantage of this method is probably that it is capable of detecting the earliest cracks of the system and their posterior growth, making possible fault detection before any other current method. The main drawback is that it requires additional transducers and a well controlled environment.

3. Experimental results

Next, the experimental test bench and acquisition system, as well as the results obtained by each of the presented fault indicators are shown, finally, two inference methods are presented to merge the obtained information.

3.1 Experimental setup

The test rig used during this research work consists of four ABB M2AA 1.1kW induction motors, three of them with the drive-end ball bearings under test (with different bearing fault degradation level), and the other one used to regulate the applied load. Both driving and loading motors were controlled using independent inverters. Motors under test have also a cable attached to the drive-end bearings housing with the other side connected to ground (a hole was mechanized in order to pass the cable through the motor shield), allowing a low resistance path for CMC acquisition proposes.

The three motors under test have *SKF 6205* bearings with normal clearance and nine balls with diameter of 7.9 mm and pitch of 38.5 mm, and a contact angle of 0.66 radians. The bearings set under test (labeled *healthy*, *lightly* and *heavily damaged*), is composed by a healthy one (with very similar vibration levels to other new units tested in previous works) and other two units with different levels of damage due their operation hours, qualitatively evaluated with a shock pulse tester from *SPM Instruments*.

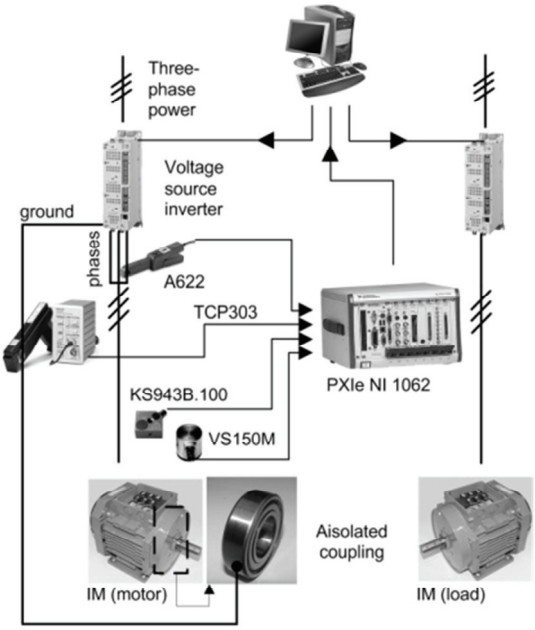

Fig. 8. Experimental test bench and acquisition system scheme.

Regarding the acquisition system, it is based on four different sensors connected to a main acquisition device. A triaxial shear design *MMF* branded piezoelectric accelerometer model *KS943B.100* with IEPE (Integrated Electronics Piezo Electric) standard output and linear frequency response from 0.5 Hz to 22 kHz, was attached using stud mounting to the drive-end motor end-shield and its data was collected at 20kS/s during 1 second for each measurement. Phase stator currents were acquired using Hall effect *Tektronix A622* probes with a frequency range from DC to 100 kHz and collected at 20 kHz during 1 second for each measurement. High frequency CMC signal was measured at the cable attached to the bearings housing with a *Tektronix TCPA300* amplifier and *TCP303* current probe, which

provides up to 15 MHz of frequency range, and acquired at 50 MHz during 100 ms for each measurement. Acoustic emissions were acquired with the use of a *Vallen-Systeme GmbH VS-150M* sensor unit with a range from 100 kHz to 450 kHz and resonant at 150 kHz. A *Vallen-Systeme GmbH AEP4 40dB* preamplifier was used before data acquisition at a sampling frequency of 25MS/s during 20ms each measurement. All the described sensors are connected to a *PXI* acquisition system from *National Instruments* formed by different specific boards.

3.2 Experimental results

3.2.1 Vibrations

The vibration signal RMS contributes clearly to bearings diagnosis. Figures 9, 10 and 11 show the evolution of the RMS value of each motor vibration signals for different speeds and load patterns tested. Clearly, the healthy motor, in figure 9, shows lower RMS values of vibration in comparison with the other two units. Figure 11, corresponding to the unit which was in the worst operational condition according to the *SPM* measurements performed, provide also the highest levels of RMS vibration values.

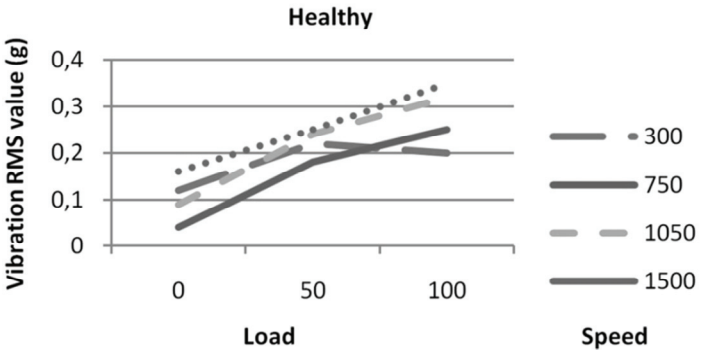

Fig. 9. RMS vibration for healthy unit, all speeds in rpm and loads in percentage of the nominal one.

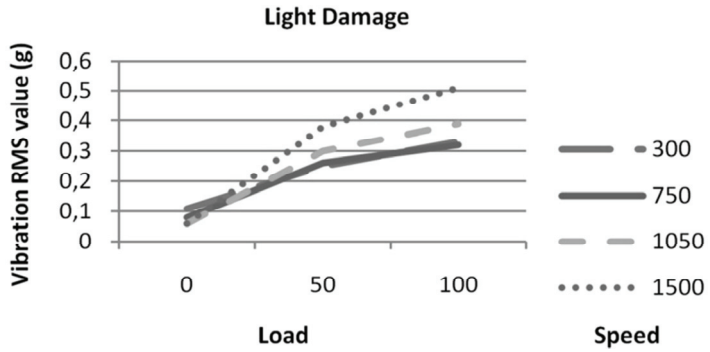

Fig. 10. RMS vibration for lightly damaged unit, all speeds in rpm and loads in percentage of the nominal one.

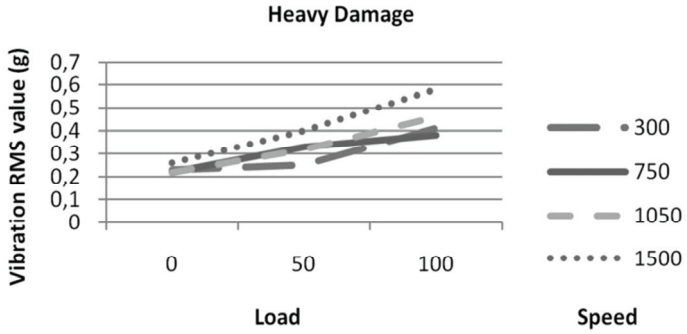

Fig. 11. RMS vibration for heavily damaged unit, all speeds in rpm and loads in percentage of the nominal one.

3.2.2 Stator currents

The figure 12a shows an example of stator-phase current in frequency domain over healthy test bench condition. The stator phase current characteristics bearing fault frequencies are related with the bearing construction parameters and the equations from (1) to (4) for m = 1 and 2 that are normally used (Obaid etal., 2003). These fault frequencies are not present along the frequency axis. The fault indicators thresholds for the stator phase current

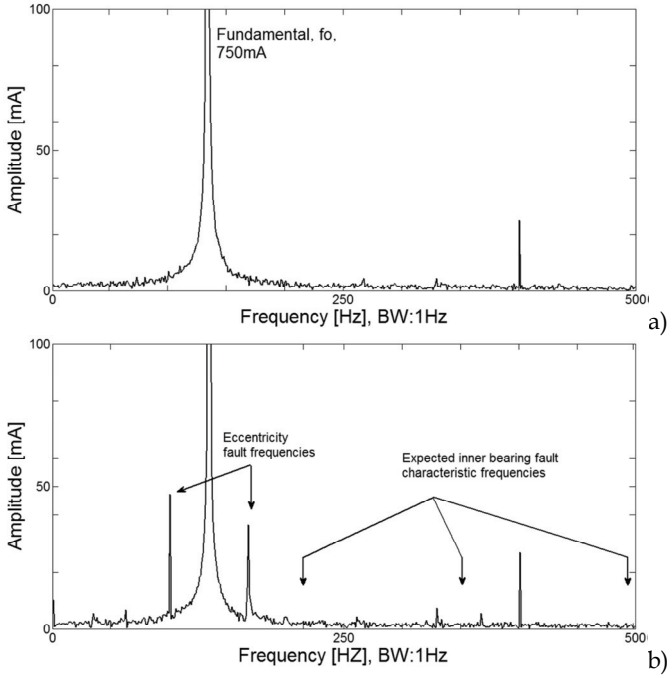

Fig. 12. Stator current frequency spectrum, from 0 to 500Hz, a) healthy bearings b) fault bearing

characteristic bearing fault frequencies can be fixed at 5% of the fundamental frequency amplitude, which is a demanding threshold for diagnosis proposes (Schoen et al., 1995). If the amplitude of these characteristic fault frequencies surpass the thresholds, imply that it can be diagnosed clearly the localized bearing fault related, but if this threshold is not surpassed for any characteristic frequency, it cannot be deduced that bearings are healthy (Zhou et al., 2009), maybe a generalized bearing defect or a non detectable single defect is occurring, then, the sidebands of the stator current fundamental harmonic will be analyzed as general eccentricity fault indicator (Bellini et al., 2008). The stator phase current spectra of a degraded bearings shows, at figure 10b, sidebands fault frequencies greater than 5% of fundamental amplitude, but there are not the characteristic bearing fault frequencies. This effect can be due to eccentricity between rotor and stator for different reasons, so it is necessary additional features in order to distinguish between eccentricity due to bearings degradation or due to other fault in the motor.

Regarding the other stator current feature presented, in order to avoid the influence of the main harmonic power value in the stator current RMS measurement, the acquired signals have been previously filtered using a band-rejection 5th order Butterworth filter centred in the power supply main harmonic with a bandwidth of 20 Hz between higher and lower cut-off frequencies. Tables 1 and 2 compare the RMS filtered values of the heavily and lightly damaged units with the healthy one.

Heavily Damaged-Healthy ([A] RMS)				
Speed [rpm] / Load [% of nominal torque]	300	750	1050	1500
0	0,004	-0,006	-0,008	-0,007
50	0,036	0,03	0,073	0,044
100	0,018	0,026	0,024	0,024

Table 1. Difference in RMS filtered current value between heavily damaged unit and healthy one used as reference.

Lightly Damaged-Healthy ([A] RMS)				
Speed [rpm] / Load [% of nominal torque]	300	750	1050	1500
0	0,008	0,002	-0,003	-0,003
50	0,002	-0,011	-0,002	-0,005
100	0,02	0,012	0,003	0,014

Table 2. Difference in RMS filtered current value between lightly damaged unit and healthy one used as reference.

A significant difference can be clearly appreciated when the motor is heavily damaged under load condition. Light damage is noticeable under nominal load conditions but its detection does not seem to be easily reliable.

3.2.3 High frequency bearings pulses

Bearings pulses threshold analysis has been executed to validate theories of correlation between bearings state (wear, lubrication, distributed defects, etc.) and pulses discharge over a threshold value. As it can be seen in figure 13 the stator CMC temporal analysis shows a decrement in the number of pulses surpassing a predefined threshold. The threshold value is fixed at 75% of the CMC pulse maximal amplitude in healthy cases. A number of counted pulses less than 75% of counted pulses in healthy bearings, will be the fault indicator threshold used to distinguish between healthy and degraded bearings.

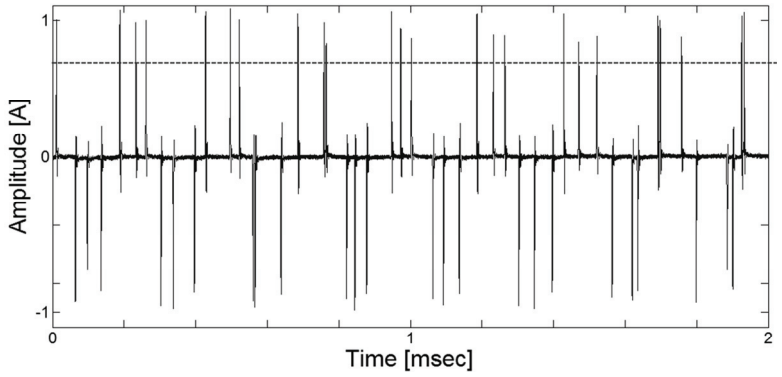

a)

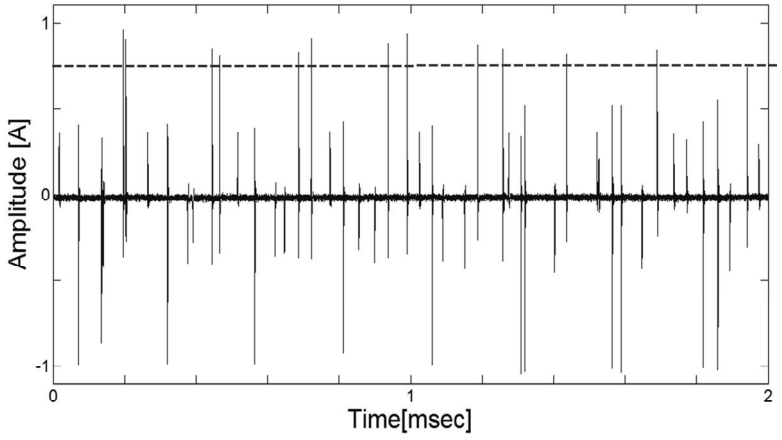

b)

Fig. 13. Example of common mode current signal acquisition, a) healthy bearings b) fault bearing.

The results summarized in figure 14, show that over a defined threshold level healthy bearings undergo a bigger number in comparison to the damaged units. It is noticeable also that this method is able to detect failure at its initial stage if the threshold is correctly placed.

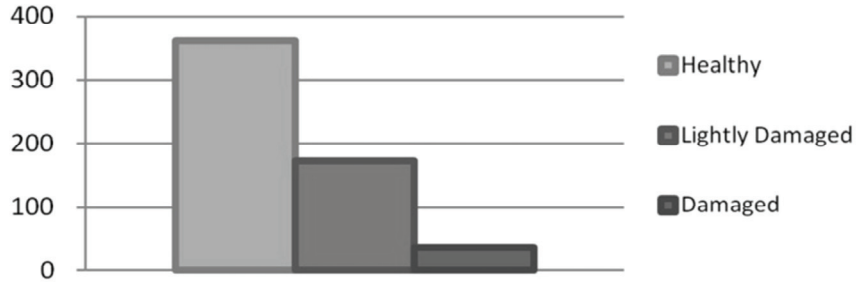

Fig. 14. Number of bearing pulses over threshold value for all motors under test. Healthy, lightly damaged and heavily damaged.

3.2.4 Acoustic Emission testing

Acoustic Emission acquired data has been statistically classified by means of value binning tools and histogram presentation. Fifteen sets of data were acquired for each motor and averaged. Figure 15 shows the results comparing the RMS voltage values acquired for the different units under test.

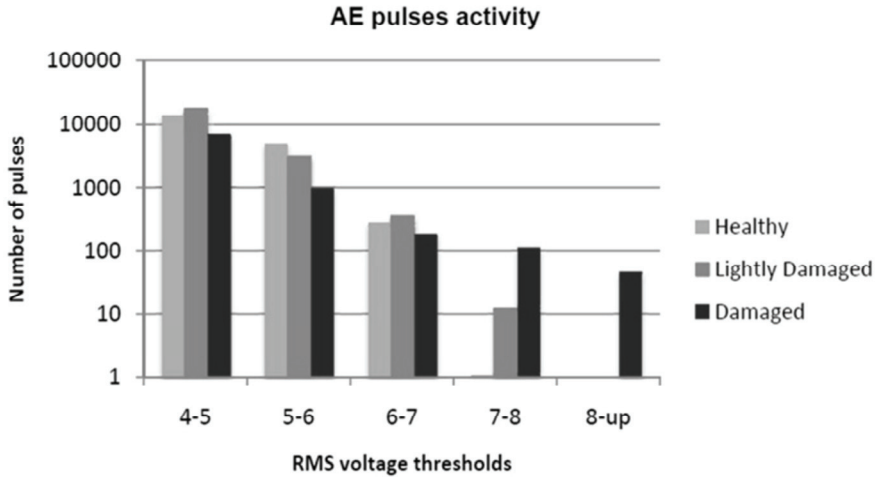

Fig. 15. Acoustic Emission voltage values classification

It is advisable that pulses over 8 V only appeared during the damaged motor testing while under 7 V that unit does not show more activity than the healthy and lightly damaged units. Then, the fuzzy inference system designed uses as reference the number of pulses that surpass the 7 V value, which is the zone where the distinction of the fault severity of the unit seemed to be more noticeable.

3.3 Inference tools

3.3.1 Look-up tables

A look-up table is a common tool applied in diagnosis field. It contents basically a set of simple association rules applied over obtained data. The operation consists in analyze a given combination of inputs in order to select one of the outputs. In the diagnosis field, this kind of inference tool is as a set of *if..then* rules collected in a table.

A proposed look-up table is shown in table 3, where a set of features, from the previously explained have been selected to generate an improved bearings diagnosis system.

FTF harmonic amplitude	BSF harmonic amplitude	BPFO harmonic amplitude	BPFI harmonic amplitude	Fundamental sidebands amplitude	Number of pulses over the threshold	Diagnosis
>5% of fundamental	Not necessary	Not necessary	Not necessary	Not necessary	< 75%	Bearing cage fault (Localized defect)
Not necessary	>5% of fundamental	Not necessary	Not necessary	Not necessary	< 75%	Bearing ball fault (Localized defect)
Not necessary	Not necessary	>5% of fundamental	Not necessary	Not necessary	< 75%	Bearing outer race fault (Localized defect)
Not necessary	Not necessary	Not necessary	>5% of fundamental	Not necessary	< 75%	Bearing inner race fault (Localized defect)
<5% of fundamental	<5% of fundamental	<5% of fundamental	<5% of fundamental	>5% of fundamental	< 75%	Bearing degradation (Distributed or non-detectable localized defect)
<5% of fundamental	<5% of fundamental	<5% of fundamental	<5% of fundamental	>5% of fundamental	< 75%	Eccentricity, but not for bearing degradation

Table 3. Look-up table considering single-point stator current characteristic harmonics, stator current fundamental frequency sidebands evaluation, and number of common mode pulses.

3.3.2 Fuzzy logic

Fuzzy logic is a useful tool in order to implement reasoning that is ambiguous or imprecise. In condition monitoring field, the implementation of tolerant and flexible rules is a more realistic way to generate a diagnosis than the use of crisp and categorical relations.

The analysis of the actual bearing status has been performed using a fuzzy logic inference implementation (Lou et al., 2004; Ballal et al., 2007), which maps given inputs (in this case current and vibration RMS values) to a single output, the different signals acquired are linked to a damage value scaled from 1 to 3.

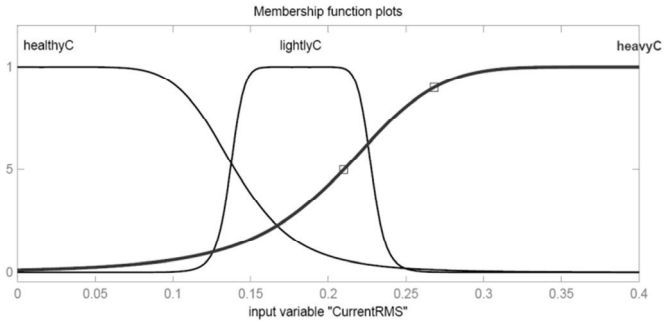

Fig. 16. Membership function plot for Current RMS. (motor speed: 1500 rpm, motor load: 0%).

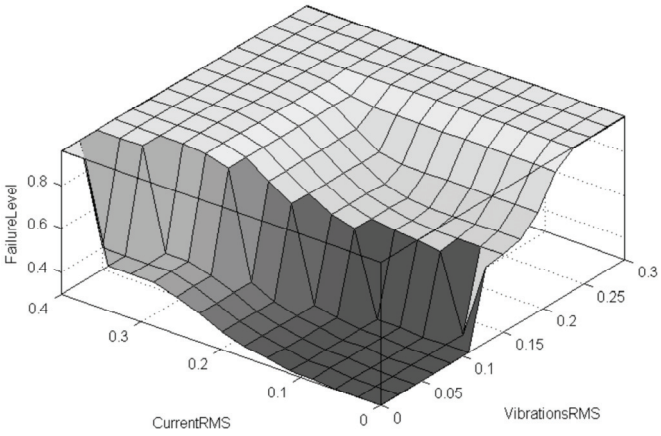

Fig. 17. Plotted surface showing the relationship between the system inputs Vibrations RMS value (g) and Stator Currents RMS value (A) versus the Failure Level output. (Motor speed: 1500 rpm, motor load: 0%)

Unit	Matches	Success %
Healthy	15	100 %
Lightly Damaged	14	93,33%
Heavy Damage	13	86,66%

Table 4. System testing results.

The membership functions, like figure 16, have been obtained through training and validation process, for each signal under analysis using real motor data. MATLAB "Adaptive neuro-fuzzy inference system" tool has been used for this purpose. Figure 17

shows the obtained relationship between Vibration and Stator Current RMS values against the Failure Level output for a motor speed of 1500 rpm and a load of 0%.
To perform the evaluation of the monitoring system designed, fifteen sets of data were collected from the same units and processed. Table 4 summarizes the obtained results.
All healthy data sets were correctly identified, whilst one of the lightly damaged was recognised as a heavily damaged set and two of the heavily damaged sets were identified as lightly damaged ones. The percentage of success was reasonably high and its improvement is still possible if more data sets are used during the system training stage.

4. Conclusions

This chapter tries to offer another point of view in the generation of diagnosis systems and the use of vibration signal analysis for machine condition monitoring. It has been presented an overview of multisensory inference approaches used to characterize motor ball bearings, and their application to a set of motors with distributed fault failure. The results show that a multivariable design contributes positively to damage monitoring of bearings, being a more solid solution than just using any of the single signals involved, which can be affected not only by external disturbances, but also by its own diagnosis limitations, especially dealing with damage severity evaluation. The selection and fusion of different fault indicators from different physical magnitudes has been solved by two examples: the application of simple look-up tables, and the development of a fuzzy system. In both proposed solutions, the bearings diagnosis reaches an important detection capability, including the possibility to detect different kinds of bearings faults and/or different levels of fault.

5. References

Ballal S., Khan Z. J., Suryawanshi H. M. & Sonolikar R. L., (2007). Adaptive Neural Fuzzy Inference System for the Detection of Inter-Turn Insulation and Bearing Wear Faults in Induction Motor, *IEEE Transactions on Industrial Electronics*, vol. 54, no. 1, pp. 250-258.

Basak D., Tiwari A. & Das S. P., (2006). Fault diagnosis and condition monitoring od electrical machines – a review, *IEEE International Conference on Industrial Technology*, pp. 3061-3066.

Bellini A., Filippetti F., Tassoni C. & Capolino G.-A., (2008). Advances in Diagnostic Techniques for Induction Machines," *IEEE Transactions on Industrial Electronics*, vol. 55, no. 12, pp. 4109-4126.

Binder A. & Muetze A., (2008). Scaling Effects of Inverter-Induced Bearing Currents in AC Machines, *IEEE Transactions on Industrial Applications*, vol. 40, no. 3, pp. 769-776.

Cabanas M. F., Melero M. G., Orcajo G. A., Cano Rodríguez J. M. & Juan Solares Sariego, (1996). Técnicas para el Mantenimiento y diagnóstico de Máquinas Eléctricas Rotativas, Marcombo, ISBN: 8426711669.

Cusido J., Delgado M., Navarro L., Sala V.M. & Romeral L., (2010). EMA fault detection using fuzzy inference tools, *IEEE AUTOTESTCON*, pp.1-6.

Cusido J., Garcia A., Navarro L. M., Delgado M., Romeral L. & Ortega A., (2009). On-line measurement device to detect bearing faults on electric motors, *IEEE Instrumentation and Measurement Technology Conference*, pp.749-752.

Cusido J., Romeral L., Delgado M., Garcia A., & Ortega J. A., (2007a). Induction machines fault simulation based on FEM modelling, *IEEE European Conference on Power Electronics and Applications*, pp.1-8.

Cusido J., Rosero J., Aldabas E., Ortega J.A. & Romeral L., (2005). Fault detection techniques for induction motors, *IEEE Compatibility in Power Electronics*, pp. 85- 90.

Cusido L. R., Garcia A., Rosero J. A. & Ortega J. A., (2007b). Fault detection in induction machines by using continuous and discrete wavelet decomposition, *IEEE European Conference on Power Electronics and Applications*, pp.1-8.

Delgado M., Garcia A., Ortega J. A., Urresty J. & Riba J. R., (2009). Bearing diagnosis methodologies by means of Common Mode Current, *European Conference on Power Electronics and Applications*, pp.1-10, 8-10.

El Hachemi Benbouzid M., (2000). A review of induction motors signature analysis as a medium for faults detection, *IEEE Transactions on Industrial Electronics,* vol. 47, no. 5, pp. 984-993.

Frosini L., Bassi E., Fazzi A. & Gazzaniga C., (2008). Use of the stator current for condition monitoring of bearings in induction motors, *Electrical Machines, International Conference on*, pp. 1-6.

Kar C. and Mohanty A. R., (2008). Vibration and current transient monitoring for gearbox fault detection using multiresolution Fourier transform, *Elsevier Journal of Sound and Vibration*, vol. 311, no. 1-2, pp. 109- 132.

Lou X., Kenneth K. A. & Loparo A., (2004). Bearing fault diagnosis based on wavelet transform and fuzzy inference, *Mechanical Systems and Signal Processing*, vol. 18, no. 5, pp. 1077-1095.

Muetze A. & Binder A., (2007). Calculation of Motor Capacitances for Prediction of the Voltage Across the Bearings in Machines of Inverter-Based Drive Systems, *IEEE Transactions on Industry Applications*, vol. 43, no. 3, pp. 665-672.

Muetze A. & Binder A., (2007). Calculation of Circulating Bearing Currents in Machines of Inverter-Based Drive Systems, *IEEE Transactions on Industrial Electronics*, vol. 54, no. 2, pp. 932-938.

O'Donell P., (1986). Report of large motor reliability survey of industrial and commercial installations, *IEEE Transactions on Industrial Applications*, vol. IA-21, no. 4.

Obaid R. R., Habetler T. G. & Stack J. R., (2003). Stator current analysis for bearing damage detection in induction motors, *Symposium on Diagnostics for Electric Machines, Power Electronics and Drives*, pp. 182-187.

Obaid, R. R, Habetler, T. G. & Stack, J. R. (2003). Stator current analysis for bearing damage detection in induction motors, *IEEE Proceeding on Power Electronics and Drives, Symposium on Diagnostics for Electric Machines*, pp. 182-187.

Riley C. M., Lin B. K., Habetler T. G. & Kliman G. B., (1999). Stator current harmonics and their causal vibrations: a preliminary investigation of sensorless vibration monitoring applications, *IEEE Transactions on Industry Applications,* vol. 35, no. 1, pp. 94-99.

Schoen R. R., Habetler T. G., Kamran F. & Bartfield R. G., (1995). Motor bearing damage detection using stator current monitoring, *IEEE Transactions on Industry Applications*, vol. 31, no. 6, pp. 1274-1279.

Singh G. K. & Saad Ahmed Saleh Al Kazzaz, (2003). Induction machine drive condition monitoring and diagnostic research-a survey, *Electric Power Systems Research*, vol. 64, no. 2, pp. 145-158.

Stack J. R., Habetler T. G. & Harley R. G., (2004). Fault Classification and Fault Signature Production for Rolling Element Bearings in Electric Machines, *Symposium on Diagnostics for Electric Machines, Power Electronics and Drives*, vol. 40, no. 3, pp. 735-739.

Zhou W., Lu B., Habetler T. G. & Harley R. G., (2009). Incipient Bearing Fault Detection via Motor Stator Current Noise Cancellation Using Wiener Filter, *IEEE Transactions on Industry Applications*, vol. 45, no. 4, pp.1309-1317.